Solvation Structure of the Ti(III) Ion in Methanol Solutions and in Perfluorinated Ionomers Swollen by Water and Methanol. A Study by ESR and ENDOR

Shulamith Schlick and Brian E. Myers*
Department of Chemistry, University of Detroit, Detroit, Michigan 48221, USA

Lars Sjöqvist and Anders Lund
Chemical Physics Laboratory, Department of Physics, Linköping University,
S-581 83 Linköping, Sweden

Z. Naturforsch. **47a,** 702–712 (1992); received January 24, 1992

The local environment of Ti^{3+} cations in methanol solutions and in Nafion perfluorinated ionomers swollen by water and methanol has been studied by electron spin resonance (ESR) and by ^1H and ^2H electron nuclear double resonance (ENDOR) spectroscopies. The two major sites reflecting the ligation of the cations as a function of solvent structure and cation concentration have been analyzed, using whenever possible the method of orientation selection for the ENDOR transitions. The distance R_N of the protons from the central cation, and the angle θ_N between the symmetry axis of Ti^{3+} and the Ti^{3+}-proton vector have been deduced by evaluating the dipolar interaction tensor and by simulating the orientation dependence of the ENDOR signal. For site 1 of Ti^{3+} in methanol ($g_{\parallel} = 1.986$ and $g_{\perp} = 1.894$) no orientation selection was possible, and R_N values in the range 4.1 to 4.6 Å are suggested from the ENDOR splittings. For site 2 of Ti^{3+} in methanol ($g_{\parallel} = 1.943$ and $g_{\perp} = 1.960$) equatorial and axial methyl protons have been detected; the R_N values deduced from the simulations are 3.95 and 4.35 Å, respectively. For Ti^{3+} in Nafion swollen by water ($g_{\parallel} = 1.997$ and $g_{\perp} = 1.907$), equatorial and axial protons from OH groups have been detected, and the ENDOR spectra were simulated with R_N values of 2.60 and 3.10 Å respectively for these protons.

I. Introduction

Electron nuclear double resonance (ENDOR) is frequently used to increase the resolution obtained in continuous wave (cw) electron spin resonance (ESR) studies of paramagnetic centers [1–4]. The method consists of monitoring the change in the intensity of an ESR transition upon scanning a radiofrequency field. In addition to increased resolution, the advantages of ENDOR are the ability to simplify the spectra, because equivalent nuclei give rise to one set of lines; to measure small hyperfine interactions that are not detected by ESR; and to deduce structural information from an analysis of matrix ENDOR signals that arise from nuclei interacting with the electron only through dipolar interaction and are situated at larger distances from the paramagnetic centers, usually > 5 Å [5].

ENDOR has been applied extensively to the study of paramagnetic centers in solutions and in single crystals. Lately, however, the method has been increasingly used in order to study paramagnetic centers in polycrystalline solids and in glasses. The most attractive and challenging feature of these studies is the ability to extract single-crystal type information, by using the method of orientation selection, which is based on measuring ENDOR responses from ESR transitions at resonant magnetic fields corresponding to specific orientations in the molecular axes system [6]. This method is possible in systems having significant g- or hyperfine anisotropy. An additional condition for obtaining single crystal-like ENDOR is that the electron cross relaxation time T_x is longer than the spin-lattice relaxation time T_{1e} of the electron spins [6]. This condition is fulfilled in many paramagnetic transition metal cations because of their short spin-lattice relaxation times. Orientation selection has been used recently to study frozen solutions of quinone anion radicals [7], to determine proton positions in polycrystalline Cu^{2+} complexes [8], and to describe the solvation of VO^{2+} in frozen methanol and water-methanol solutions [9] and in vanadyl phosphate pentahydrate [10].

In a previous study we have used ENDOR for the study of the local structure of Ti^{3+} in the perfluori-

---

* Undergraduate research fellow.

Reprint requests to Shulamith Schlick, Department of Chemistry, University of Detroit, Detroit, Michigan 48221, USA.

0932-0784 / 92 / 0500-0702 $ 01.30/0. – Please order a reprint rather than making your own copy.

nated membranes known as Nafion, swollen by CH_3OH and selectively deuteriated methanols [11]. A distance of 8.0 ± 0.3 Å between the cation and the closest fluorine nuclei of the network has been deduced from an analysis of the matrix ENDOR ^{19}F signals, and a distance of 4.3 Å between the cation and the methyl protons of the methanol closest to the cation.

In this paper we present ENDOR studies of the Ti^{3+} center in methanol solutions and in perfluorinated ionomers swollen by water and methanol. The motivation for the present study was our interest to use orientation selection to obtain maximum resolution in ENDOR spectra; to detect differences in the local environment of the paramagnetic cation in solutions and in the ionic domains of the ionomers; and finally to characterize in greater detail the two major sites obtained in ESR studies of Ti^{3+} in frozen methanol solutions and in the ionomer swollen by water and methanol [12]. The complex chemistry of Ti^{3+}, a d^1 spin system, and the very few ENDOR studies for the cation provided additional motivation [13–17]. By contrast, ENDOR of VO^{2+} complexes, containing the d^1 V^{4+} ion, has been extensively studied in single crystals and in frozen solutions [9, 10, 18, 19].

II. Experimental Section

The Nafion 117 sulfonated membranes, with an equivalent weight of 1100 g/mole SO_3H and a thickness of 0.178 mm were obtained from DuPont. The formula for the acid form (NafionH) is given below.

NafionH, n=1

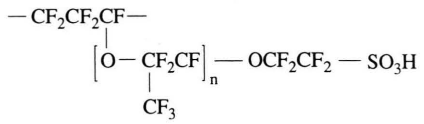

$$\begin{array}{l} -CF_2CF_2CF- \\ \qquad\qquad | \\ \qquad\quad \left[O-\underset{\displaystyle CF_3}{\underset{|}{CF_2CF}}\right]_n-OCF_2CF_2-SO_3H \end{array}$$

Scheme 1

The membranes were pretreated as described in our previous publications [11, 12, 20–22] and dried to constant weight in vacuo (10^{-4} torr) for 24 h at ambient temperature and for 2–12 h at 373 K. $TiCl_3$ (Aldrich) was used as received to prepare water and methanol solutions under dry nitrogen. Doubly distilled deionized water was used in all experiments. Methanol (Fisher) and deuteriated methanols (Norell) were dehydrated by using molecular sieves type 3 A from Kodak. The deuterium enrichment of CH_3OD and D_2O was at least 99%. Methanol and water solutions of $TiCl_3$ in the concentration range 0.04–0.10 M were used to exchange the SO_3H groups of the dried ionomer, based on three sulfonate groups per Ti^{3+}.

ESR spectra at X-band were measured with a Bruker 200D SRC spectrometer operating at 9.7 GHz (empty cavity at ambient temperature), interfaced with a data system based on an IBM PC and the software EPRDAS (Mega Systems Solutions, Rochester, New York). The microwave frequency was measured with the HP 5342A frequency counter. The absolute value of the magnetic field was measured with a Micro-now gaussmeter model 515B and with 2,2-diphenyl-1-picrylhydrazyl (DPPH, $g = 2.0036$) and Cr^{3+} in a single crystal of MgO ($g = 1.9796$). ENDOR spectra were measured at 9.36 GHz on a Bruker 200D spectrometer equipped with the Aspect 2000 computer, using an rf modulation depth of 90–125 kHz and a maximum rf power of 100 watts. For lower modulation frequencies the signal intensity decreased but the line widths were unchanged. The magnetic field was measured with the Bruker ER 035 NMR Gaussmeter, and the microwave frequency was measured with an EIP model 548 A frequency counter. In all ENDOR experiments helium was used as the coolant in a flow cryostat from Oxford instruments. Spectra were simulated by an HP Vectra RS/20C computer equipped with a 386 processor, using codes written in Turbo Pascal 5.0 [23].

III. Results

III.1 Ti^{3+} Solutions in Methanol

ESR Spectra: Normally only g-anisotropy is observed in ESR spectra of Ti^{3+} centers, because the most abundant ^{48}Ti isotope has $I = 0$ (natural abundance 73.94%). The isotopes with non-zero magnetic spins are ^{47}Ti ($I = 5/2$) and ^{49}Ti ($I = 7/2$), with natural abundances 7.28 and 5.51%, respectively. Signals from these isotopes were detected in ESR spectra at high gain and above 225 K, because the line widths are narrowed due to dynamical processes [22]. X-band ESR spectra at 77 K for two $TiCl_3$ concentrations in CH_3OD are shown in Figure 1. Two major sites are detected as a function of cation concentration. For site 1, $g_{\parallel} = 1.986$ and $g_{\perp} = 1.894$; these values are typical of Ti^{3+} ligated to six oxygen ligands in a trigonally distorted octahedral symmetry, such as titanium

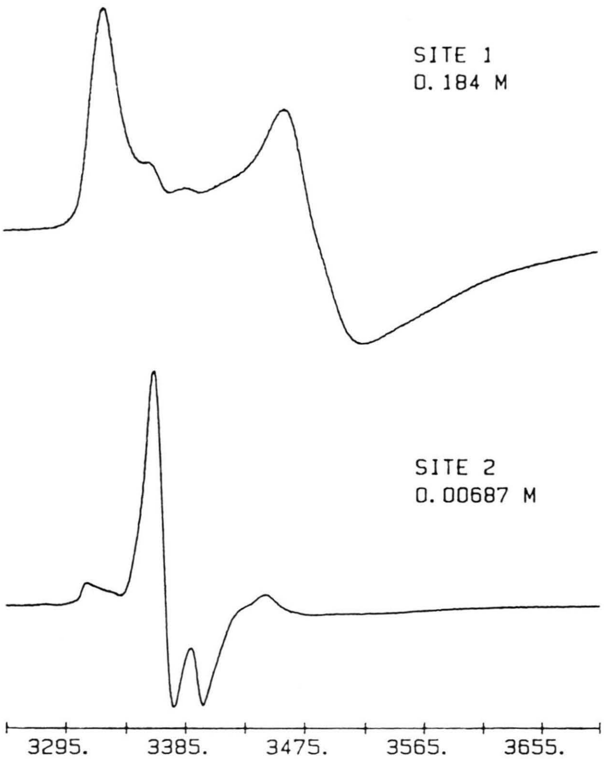

Fig. 1. X-band ESR spectra (microwave frequency 9.35 GHz) at 77 K of Ti^{3+} in CH_3OD, for the indicated cation concentrations.

acetylacetonate [24a]. For site 2, $g_{\parallel} = 1.943$ and $g_{\perp} = 1.960$, typical of a tetragonally distorted octahedral symmetry with $\Delta \gg \delta \gg \lambda$. Here Δ is the cubic field splitting of the d^1 ion, δ is the tetragonal distortion and λ is the spin-orbit coupling constant, 154 cm^{-1} for Ti^{3+} [24b]. The symmetries of the two sites are shown in Scheme 2. The g-values for site 1 are similar to those measured for Ti^{3+} in the perfluorinated membranes swollen by methanol, 1.989 and 1.878, respectively [12]. The slight variations in the g-values for these systems are not surprising, because in methanol solutions Cl^- ions are present; in Nafion however the concentration of Cl^- is negligible (11 ppm in dry Nafion), due to the low anion permeability of the membranes. Moreover, in Nafion oxygen ligands from the sulfonic group of the network are available, in addition to oxygen ligands from the solvent. In the membranes both sites are detected in a wide range of cation concentrations, with site 1 dominant at high, and site 2 at low, degree of neutralization of the membranes.

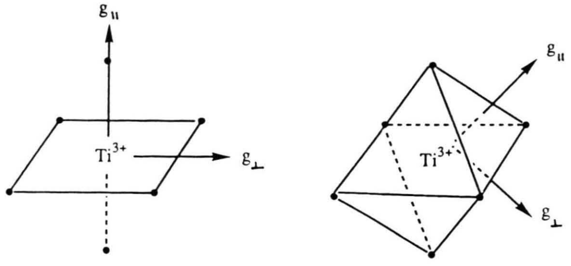

Tetragonally Distorted Octahedron
(Site 2)

Trigonally Distorted Octahedron
(Site 1)

Scheme 2

ENDOR Spectra, Site 1: ENDOR spectra from site 1 of Ti^{3+} in CH_3OH and CH_3OD at 4 K, with the magnetic field at the perpendicular and parallel positions are shown in Figure 2. No change in line positions and only small changes in the relative intensities of the lines are detected in ENDOR spectra recorded at 10 K and 20 K. Deuteriation of the solvent has no effect on the spectra, and indicates that all signals are due to the methyl protons. No significant difference in the spectra as a function of field setting is detected. For the parallel orientation pairs of lines separated by 1.81 MHz and 0.64 MHz are detected; a weak shoulder with a splitting of 2.50 MHz is also measured. The corresponding splittings for the perpendicular direction are 1.73, 0.56 and 2.38 MHz. The splittings are summarized in Table 1. Splittings from the OH protons are not detected in the frequency range defined in Figure 2. ENDOR results obtained from Ti^{3+} in Nafion swollen by H_2O and CH_3OH indicate that signals from OH protons are hard to detect, as seen below and in Figure 5.

ENDOR Spectra, Site 2: ENDOR spectra from site 2 of Ti^{3+} in CH_3OH and CH_3OD, with the magnetic field set at the perpendicular and parallel positions, are shown in Figure 3. All spectra are at 4 K except that in Fig 3C, which is at 10 K; only slight differences in line intensity and no effect on line positions is detected at this temperature, compared to 4 K. It is clear that the splittings are due to the methyl protons. For the parallel orientation hyperfine splittings of 1.74 and 0.40 MHz are measured, and for the perpendicular orientation the splittings are 3.12, 1.42 and 0.42 MHz, all within ± 0.02 MHz. ENDOR spectra measured with the magnetic field parallel and perpendicular to the symmetry axis of the Ti^{3+} complex are different, indicating orientation selection. The splittings are given in Table 1.

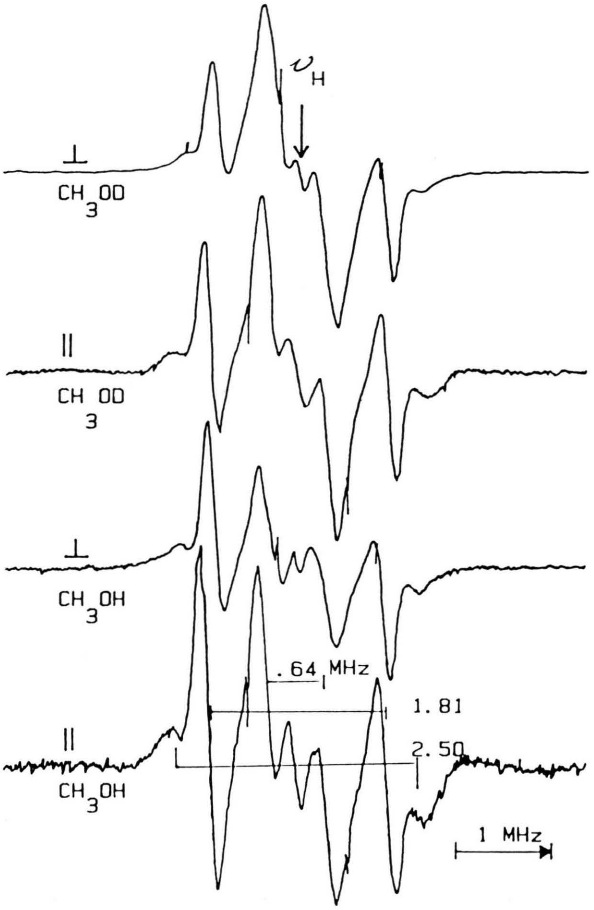

Fig. 2. ENDOR spectra at 4 K from site 1 of Ti^{3+} in methanol (CH_3OH and CH_3OD), for parallel and perpendicular field settings, as indicated. Downward arrow labelled ν_H indicates the proton Zeeman frequency.

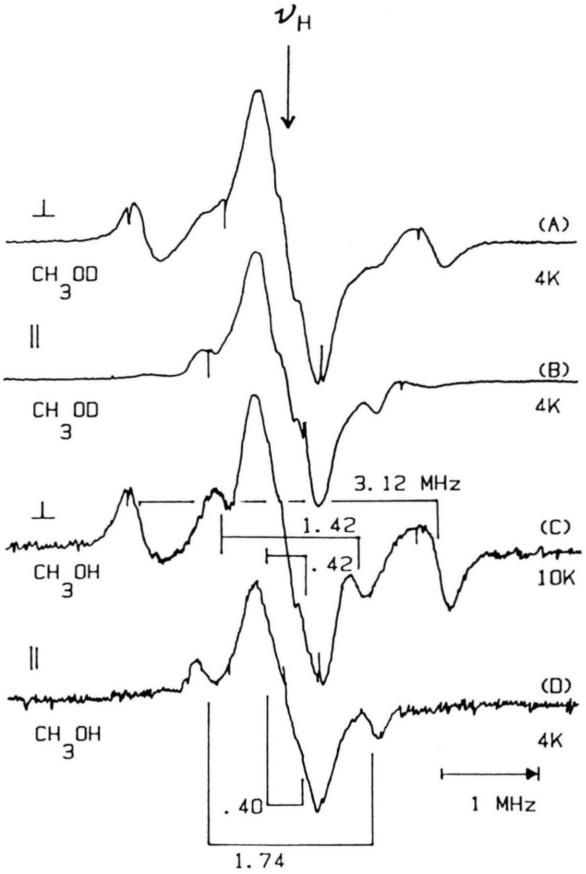

Fig. 3. ENDOR spectra from site 2 of Ti^{3+} in methanol (CH_3OH and CH_3OD), for parallel and perpendicular field settings, as indicated. All spectra are at 4 K, except in (C), which is at 10 K. Downward arrow labelled ν_H indicates the proton Zeeman frequency.

III.2 Ti^{3+} in Nafion Swollen by Water

In Nafion swollen by water only site 1 is detected, with $g_{\parallel} = 1.997$ and $g_{\perp} = 1.907$. ENDOR spectra at 4 K for Ti^{3+} in Nafion swollen by H_2O, for the field settings indicated in the inset, are shown in Figure 4. The ^{19}F matrix line is observed in all spectra and is indicated by the arrow. The main splittings detected in the parallel orientation are 4.9 and 0.75 MHz. The intensity of the outer doublet decreases when the magnetic field is increased, away from the parallel orientation. For field position ***d*** a pair of lines with a splitting of 3.35 MHz is detected. Also visible for the perpendicular orientation (field positions ***c*** and ***d***) is the

Table 1. Proton hyperfine splittings of ENDOR spectra for Ti^{3+} in methanol and in Nafion swollen by water or methanol.

System	ENDOR splittings (MHz)	Field set
Ti^{3+}/Methanol		
site 1	1.73, 0.56, 2.38	$g_{\perp} = 1.894$
	1.81, 0.64, 2.50	$g_{\parallel} = 1.986$
site 2	3.12, 1.42, 0.42	$g_{\perp} = 1.960$
	1.74, 0.40	$g_{\parallel} = 1.943$
Ti^{3+}/Nafion/Water		
site 1	3.35, 1.35, 0.60	$g_{\perp} = 1.907$
	4.90, 0.75	$g_{\parallel} = 1.997$

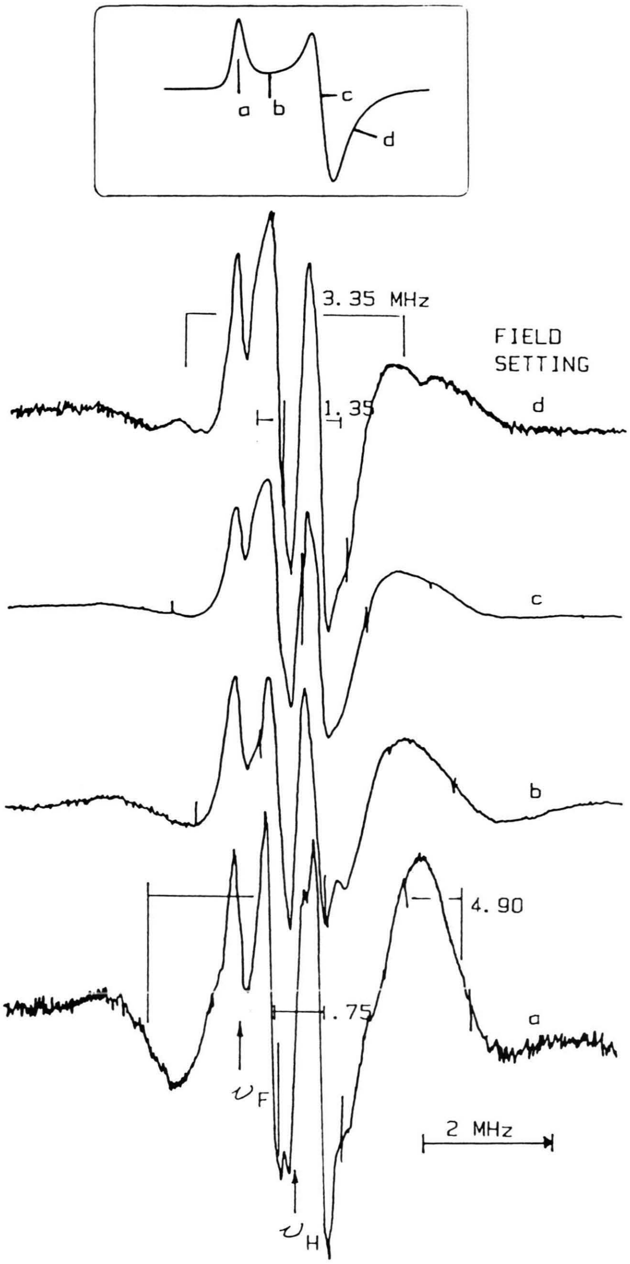

Fig. 4. ENDOR spectra at 4 K from Ti^{3+} in Nafion swollen by H_2O, for the field settings indicated in the ESR spectrum of the inset. Upward arrows labelled ν_H and ν_F indicate the proton and fluorine Zeeman frequencies.

shoulder corresponding to a splitting of 1.35 MHz and the inner pair with a splitting of 0.5–0.7 MHz. The splittings are given in Table 1.

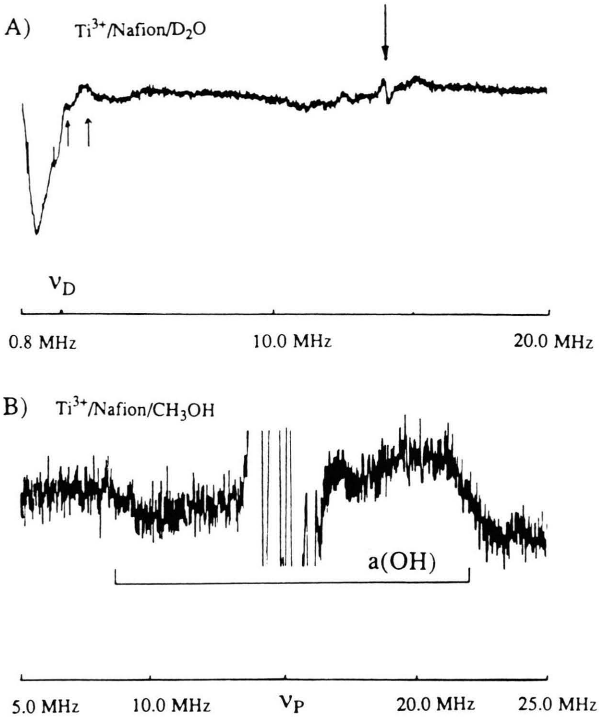

Fig. 5. (A) ENDOR spectrum at 4 K of Ti^{3+} in Nafion swollen by D_2O. Downward arrow indicates the fluorine nuclear frequency; upward arrows indicate deuterium signals. (B) ENDOR spectrum of Ti^{3+} in Nafion swollen by CH_3OH, indicating the broad signals assigned to the equatorial proton (from OH). Both spectra are obtained for the perpendicular field setting.

For Ti^{3+} in Nafion swollen by D_2O and with the field set at the perpendicular orientation (Fig. 5A) the fluorine matrix line is dominant in the region of the ^{19}F and ^{1}H nuclear frequencies. A broad signal is detected at ≈ 1.1 MHz from the deuterium nuclear frequency ν_D, corresponding to a hyperfine splitting of ≈ 14 MHz for protons; this splitting is assigned to the equatorial proton of the OH group. A weaker signal is observed at ≈ 0.25 MHz from ν_D, corresponding to a proton splitting of 3.5 MHz, and is identified with the proton splitting detected in Fig. 4, for field position ***d***.

We were not able to detect the large splittings predicted for OH protons in Nafion swollen by H_2O, even for high gain. For Ti^{3+} in Nafion swollen by CH_3OH, however, a pair of weak and broad lines separated by ≈ 13.5 MHz is detected, with the field along the perpendicular orientation, and is shown in Fig. 5B; the signals from the methyl protons are well out of scale. Large proton splitting were not detected with the field along the parallel direction. Methyl protons and ^{19}F nuclei have smaller splittings and line widths. From these spectra we conclude that the broad signals are due to OH protons which have large splittings for the perpendicular orientation, but are hard to detect, because of the large signal width.

These conclusions are in agreement with results obtained by several groups. Mustafi and Makinen detected very weak but large (15.67 and 13.38 MHz) proton splittings for the perpendicular direction of VO^{2+} in frozen methanol solutions [9]. Gourier et al. measured a deuterium splitting corresponding to a proton splitting of 16.9 MHz for Ti^{3+} sandwich compounds in organic glasses but were unable to detect the proton signals [16, 17]. Finally, we detected deuterium signals for Ti^{3+} in Nafion swollen by CD_3OD that correspond to a proton splitting of 15.6 MHz [11]. These effects are due to the large range of splittings for these protons; in support of this logic are the recent results of Gourier et al., which indicate larger amplitudes, and narrower lines, for the signals when the temperature is raised, and averaging of the inhomogeneities and anisotropies sets in [17].

Large splittings from OH protons are also suggested in ESR spectra of Ti^{3+} in deuteriated solvents. ESR spectra of Ti^{3+} in Nafion swollen by selectively deuteriated methanols indicate narrower line widths in the fully deuteriated solvent CD_3OD. The widths at half maximum height of the parallel signal increase with progressive deuteriation, and are 5.0, 5.5, and 6.5 G for CD_3OD, CH_3OD and CH_3OH, respectively; the signals in the perpendicular region of the ESR spectra are particularly affected by deuteriation. This result is in agreement with the ENDOR detection of the large splitting from the OD deuteron when this orientation was selected. These ESR spectra suggest that CH_3 and OH protons contribute to the line widths for this orientation.

IV. Simulation of the ENDOR Spectra

Because the anisotropy of the proton hyperfine tensor is due to an approximate point dipolar interaction, the principal values of the proton hyperfine tensor, $A_{\parallel}$ and $A_{\perp}$, are respectively parallel and perpendicular to the electron-proton direction. Therefore the principal axes systems for the **g**-tensor and for the hyperfine tensor are in general not colinear. Orientation selection is possible if the electron-nucleus vector R_N is along, or very close to, one of the principal axes of the **g**-tensor. For this case, and for a field setting along the axial direction ($g_{\parallel}$), it is possible to obtain ENDOR signals corresponding to the parallel hyperfine tensor component of axial nuclei, $A_{\parallel}$ (axial), and to the perpendicular hyperfine component of equatorial nuclei, $A_{\perp}$ (eq). Similarly, for a field setting along $g_{\perp}$, it is possible to measure $A_{\parallel}$ (eq), $A_{\perp}$ (eq), and $A_{\perp}$ (axial) [8, 9].

The geometry for nuclei at arbitrary orientations to the principal values of the axial **g**-tensor is shown in Scheme 3, where $g_1 = g_2 = g_{\perp}$, and $g_3 = g_{\parallel}$. For each field setting (expressed as θ_H), an ENDOR signal that is a summation over all angles ϕ_H is obtained; this summation leads to powder type ENDOR signals even when $T_x > T_{1e}$ [8].

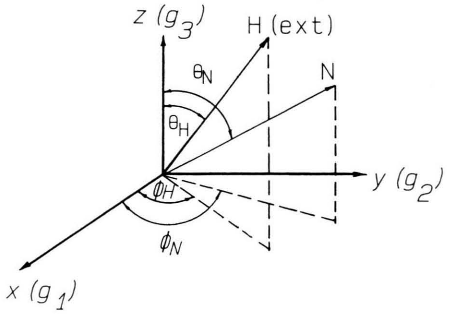

Scheme 3

In order to deduce the details of the structure and ligation, it is therefore necessary to simulate the spectra, starting with values suggested by inspection of the experimental ENDOR spectra. The parameters needed for the simulations are $g_{\parallel}$, $g_{\perp}$, the cation-proton distance R_N, the angles θ_N and ϕ_N that define the proton orientation in the axes system of the **g**-tensor, and the isotropic hyperfine coupling A_{iso}. The ENDOR spectrum (intensity as a function of the rf frequency) for a given field orientation θ_H was calculated from the following equations [8]:

$$r_1 = \sin\theta_N \cos\phi_N, \quad r_2 = \sin\theta_N \sin\phi_N, \quad r_3 = \cos\theta_N, \tag{1}$$

$$h_1 = \sin\theta_H \cos\phi_H, \quad h_2 = \sin\theta_H \sin\phi_H, \quad h_3 = \cos\theta_H, \tag{2}$$

$$A_{ij} = -(\beta_e \beta_N g_N / h R_N^3)\, g_i (3 r_i r_j - \delta_{ij}) + A_{iso}, \tag{3}$$

$$v(\theta_H) = \sum_{\phi_H=0}^{2\pi} \sum_{m_s=-1/2}^{1/2} \left[\sum_{i=1}^{3} \left[\frac{m_s}{g(\theta_H, \phi_H)} \cdot \left(\sum_{j=1}^{3} g_j h_j A_{ji} \right) - h_i v_0 \right]^2 \right]^{1/2}. \tag{4}$$

In eq. (1) to (4) β_e, β_N, and g_N have the usual meaning, and ν_0 is the proton Zeeman frequency at the field setting of the ENDOR experiment. The signal was convoluted with a line shape function consisting of a linear combination of Lorentzian and Gaussian line shapes with coefficients chosen to obtain the best visual fit with experimental results; the derivative of the signal is then plotted.

V. Discussion

In this section we will determine the principal values and directions of the hyperfine tensors for protons and the electron-proton distances, based on the experimental ENDOR spectra; simulations of orientation dependent spectra will provide an additional verification. The results will then be discussed in order to deduce the local environment of the Ti^{3+} cations in frozen solutions and in Nafion swollen by water and methanol.

V.1 Ti^{3+} in Methanol

Site 1: The major splittings of 1.81 and 0.64 MHz can be interpreted as in our previous study [11], as a hyperfine tensor (1.81, −0.64, −0.64) MHz, $A_{iso} = 0.18$ MHz and a dipolar tensor (1.63, − 0.82, − 0.82) MHz, leading to $R_N = 4.6$ Å. The largest splitting measured is 2.5 MHz; if we assume that the three protons of the methyl group have similar values of A_{iso} and that the value of 2.5 MHz represents a maximum value of the hyperfine tensor for one of the protons (the closest to the cation), the largest dipolar coupling for these protons is 2.32 MHz. This procedure leads to an R_N value of 4.1 Å for this proton. Both R_N values are similar to the R_N values for the equatorial and axial protons in site 2 (4.0 and 4.2 Å, see below), and to that for site 1 in Nafion swollen by methanol, where a distance of 4.3 Å was deduced, in a similar fashion [11]. The shape of the lines split by 1.81 MHz with the field set at $g_{\|}$ does not have the appearance of a genuine parallel ENDOR absorption of the type previously reported [8, 9]. One possible explanation is that the principal axes of the **g**- and the hyperfine tensors do not coincide for site 1. Another possibility is that this is an $A_{\perp}$ component from some other proton. Numerous simulations were performed, but in the absence of orientation selection it is not possible to obtain an unique set of parameters by simulation of ENDOR spectra. The assignment therefore remains tentative.

Site 2: The results presented in Fig. 3 for the methyl proton splittings in site 2 of Ti^{3+} in methanol can clearly be assigned to contributions from the axial protons with $A_{\|}$ (axial) = 1.74 MHz (Fig. 3 B) and the equatorial protons with $A_{\|}$ (eq) = 3.12 MHz (Figure 3 A). The shoulders on the central line of Fig. 3 A are attributed to the axial protons with $|A_{\perp}\text{(axial)}| =$ 1.4 MHz. A value of $|A_{\perp}\text{(eq)}| = 0.4$ MHz is estimated from the poorly resolved features of the central line in Figs. 3 A and 3 B. The shoulder features of Fig. 3 A are enhanced when CH_3OH is used as solvent, Figure 3 C. In this case, however, one cannot exclude that features from the OH protons may distort the line shape. The assignment is therefore made on the basis of the spectra in Figs. 3 A and 3 B. The simulations are described below. By choosing negative signs for $A_{\perp}$ the following dipolar tensors are obtained, (2.35, −1.17, −1.17) and (2.09, −1.05, −1.05) MHz, corresponding to $R_N = 4.0$ and 4.2 Å for the equatorial and axial protons, respectively. A positive value for $A_{\perp}$ gives a larger than expected R_N value of 9 Å for the axial protons, and an R_N value for the equatorial protons larger than for the axial protons, which is not acceptable for the symmetry of the system.

The clear orientation selection observed in the experimental spectra greatly facilitated the simulation process; excellent agreement with the experiment is seen in Fig. 6, for the parallel and perpendicular field settings, with $A_{iso}\text{(axial)} = -0.25$ MHz, $R_N\text{(axial)} =$ 4.35 Å, $A_{iso}\text{(eq)} = 0.70$ MHz and $R_N\text{(eq)} = 3.95$ Å. The simulated spectra were obtained by adding the contribution of a matrix proton with $\theta_N = 45°$ and at a distance of 7.4 Å from the central cation. The separate contributions of the three types of protons (axial, equatorial and matrix), for the parallel and perpendicular field settings are given in Figs. 6 A and 6 B. The experimental dipolar tensors, the deduced R_N values, and the simulated parameters for site 1 and 2 (Ti^{3+}/methanol) are summarized in Table 2.

The difference in the sign of A_{iso} for the two types of protons deserves a comment. The ENDOR measurements do not yield the sign of the hyperfine coupling. The signs may be theoretically predicted for simple cases such as conjugated free radial systems (cf. Chap. 6 and 8 of [24]). For solvated electron system, OH protons have positive and CH_3 protons have negative sign of A_{iso} [26]. In the present case the sign cannot be easily predicted without detailed calculations. In the analysis of experimental data the signs of the tensor components were chosen to give physically reasonable

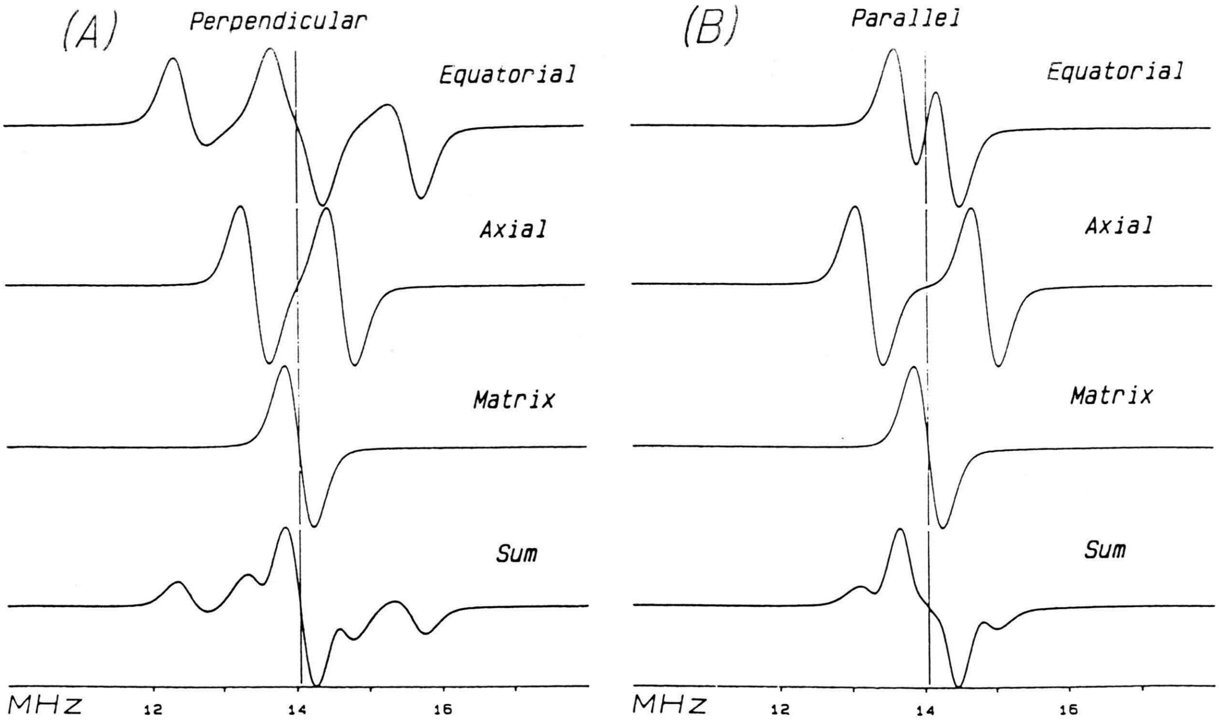

Fig. 6. Simulation of the ENDOR signals given in Fig. 3 (site 2 in Ti^{3+}/methanol) with line shapes that are a combination of Lorentzian and Gaussian functions with equal coefficients, and a line width of 0.25 MHz. The equatorial proton is at 3.95 Å, with $A_{iso} = 0.70$ MHz; the axial proton is at 4.35 Å, with $A_{iso} = -0.25$ MHz; the matrix proton is at 7.40 Å and $\theta_N = 45°$. (A) Separate contributions of the protons and the sum for the perpendicular field setting ($\theta_H = 90°$). (B) Separate contributions of the protons and the sum for the parallel field setting ($\theta_H = 0°$). In calculating the final spectra, the intensity ratio of the equatorial, axial and matrix protons is 1:0.25:0.4.

Table 2. Experimental dipolar hyperfine tensors, parameters used in the simulations, and evaluated R_N values for Ti^{3+} in methanol and Nafion swollen by water and methanol.

System	Dipolar tensor (MHz)	Proton	R_N (Å)	A_{iso} (MHz)
Ti^{3+}/Methanol				
site 1	(1.63, −0.82, −0.82)[a]		4.6	0.18
	(2.32, −1.16, −1.16)[a]		4.1	0.18
site 2	(2.35, −1.17, −1.17)	(eq)	4.0	0.77
	(2.09, −1.05, −1.05)	(axial)	4.2	−0.35
simulated				
		(eq)	3.95	0.70
		(axial)	4.35	−0.25
Ti^{3+}/Nafion/Water				
site 1	(5.5, −2.75, −2.75)	(axial)	3.1	−0.60
	(9.8, −4.9, −4.9)	(eq)	2.5	4.2
	(8.9, −4.45, −4.45)	(eq)	2.6	5.1
simulated				
		(axial)	3.10	−0.60
		(eq)	2.60	5.10

[a] No orientation selection.

Ti^{3+}-proton distances, and to obtain a positive sign for $A_{\parallel}$, as predicted from Eq. (2) when $A_{iso} = 0$.

V.2 Ti^{3+} in Nafion Swollen by Water

The most logical choice for the hyperfine components of the axial protons is (4.90, −3.35, −3.35) MHz, leading to an isotropic component of −0.60 MHz and a dipolar tensor of (5.5, −2.75, −2.75) MHz, and to $R_N = 3.1$ Å. Another possibility is to choose the tensor components (4.90, −1.35, −1.35), leading to a dipolar tensor (4.17, −2.08, −2.08) MHz and $R_N = 3.4$ Å. We prefer the first choice, because of the clear appearance of the splitting of 3.35 MHz at field setting ***d*** in Fig. 4, where it is most likely that only the perpendicular orientation has been selected. This is the result given in Table 2. The shoulder separated by 1.35 MHz might be due to protons in the second solvation shell. For the equatorial proton the choices are (14.0, 0.7, 0.7) or (14.0, −0.7, −0.7) MHz which correspond to the following dipolar tensors (8.9, −4.45, −4.45) and

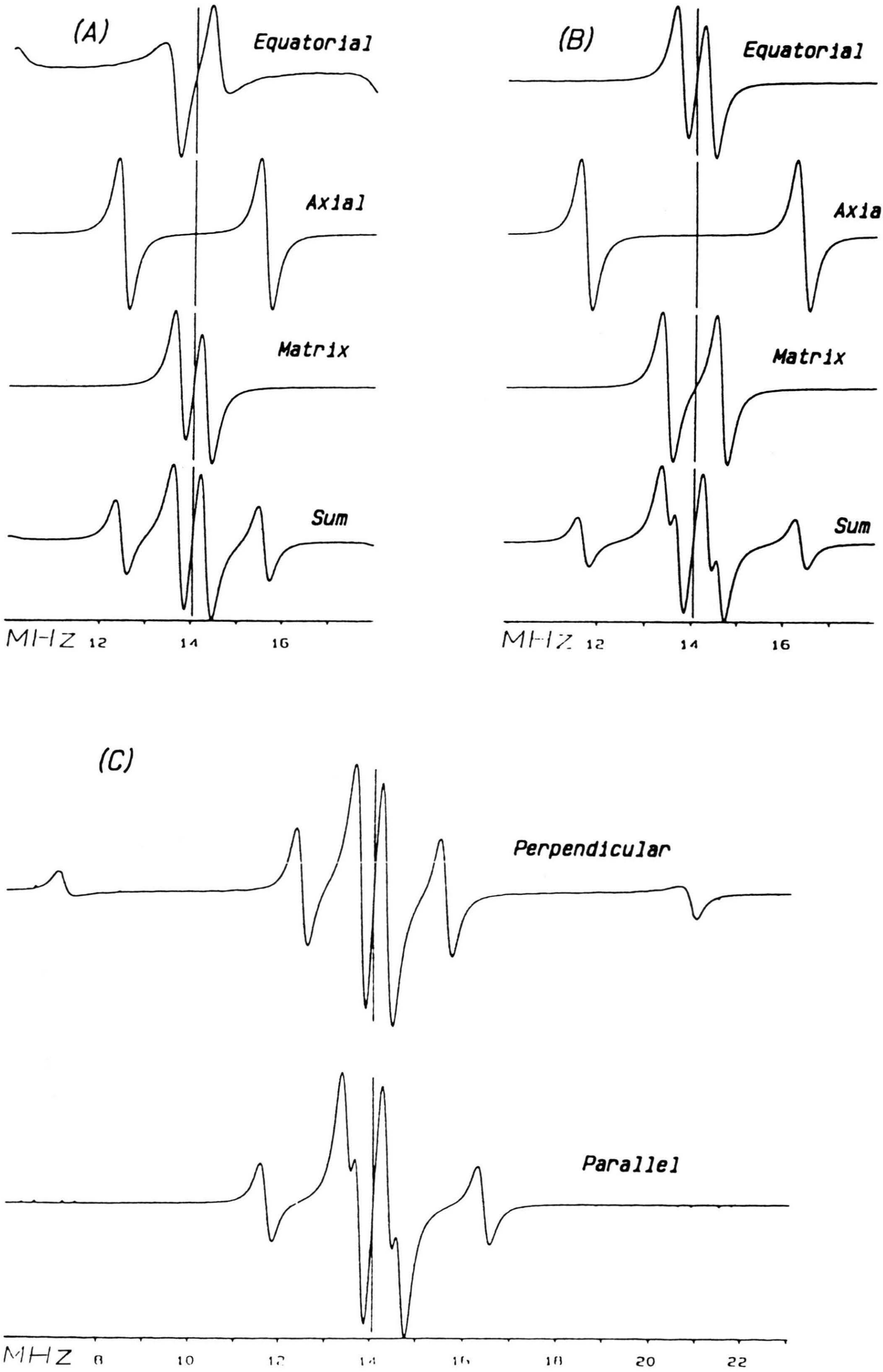
(A)
Equatorial
Axial
Matrix
Sum
MHZ 12
14
16
(B)
Equatorial
Axial
Matrix
Sum
MHZ 12
14
16
(C)
Perpendicular
Parallel
MHZ 8
10
12
14
16
18
20
22

(9.8, −4.9 −4.9) MHz, leading to R_N values of 2.6 and 2.5 Å, respectively. These values are in the range of distances deduced for the equatorial protons in $VO(H_2O)_5^{2+}$, in ENDOR studies of single crystals [18]. The very large anisotropy for these protons is comparable to that of trapped electrons interacting with hydroxyl protons in polyhydroxy compounds [25, 26].

Simulated spectra are presented in Figs. 7A and 7B for the $\theta_H = 90°$ and $\theta_H = 0°$ field directions, and the proton parameters $A_{iso}(eq) = 5.1$ MHz, $R_N(eq) = 2.60$ Å, and $A_{iso}(axial) = -0.60$ MHz and $R_N(axial) = 3.1$ Å. A matrix proton at 5.1 Å and $\theta_N = 0°$ was introduced, to improve the fit. The contribution of each type of proton and the sum is shown in Figs. 7A and 7B, for the two field settings. While the position of the lines is in excellent agreement with experimental spectra, the outer signals in the experimental spectra in Fig. 4 are much broader, suggesting a distribution of sites differing in the bonding parameters. In Fig. 7C we present the simulated spectra for the perpendicular and parallel field settings, on a wide frequency scale. We note that the large splitting in Fig. 7C at $\theta_H = 90°$ is not detected experimentally. The dipolar tensors and the parameters used in the simulations are given in Table 2.

V.3 Local Environment of Ti^{3+} in Methanol and in Swollen Nafion

The ESR spectra presented in Fig. 1 indicate different solvation schemes of Ti^{3+} in methanol, depending on the cation concentration. For site 2 of Ti^{3+} in methanol, which is predominant at low cation concentration, axial and equatorial methyl groups are detected in ENDOR spectra. Excellent agreement between simulated and experimental spectra has been obtained when the intensity ratio of equatorial to axial protons is 4:1. If we assume that the two types of protons have a similar relaxation behaviour, this ratio suggests a total of five oxygen ligands from methyl groups, four in the equatorial plane and one along $g_{\parallel}$. This is in agreement with other ESR studies of Ti^{3+} that suggest ligation of five methanol molecules to Ti^{3+} at low cation concentrations, when the ratio of solvent molecules to cations is very high [27]. The site has a tetragonally distorted octahedral symmetry.

For site 1 of Ti^{3+} in methanol, which dominates at higher cation concentrations, Ti^{3+}-proton distances are in the range 4.1−4.6 Å. NMR studies of concentrated methanol solutions of Ti^{3+} suggest an average coordination number of 4 methanol groups [28]. We have no way to verify this conclusion by simulations. For Ti^{3+} in Nafion swollen by methanol both sites are detected in a wide range of concentrations, with site 1 dominant at high degree of neutralization of the membrane. Site 1 most likely represents the cation ligated to oxygens from the methanol and, in addition, to the sulfonic groups of the network. This conclusion is in agreement with our previous results for Ti^{3+} in methanol containing isethionic acid CF_3SO_3, where site 1 is dominant [12]. It appears that in Nafion swollen by methanol the preferred ligation of the cation is to the oxygen ligands from the network, in addition to solvent molecules.

In Nafion swollen by water Ti^{3+} in site 1 only is detected. If we assume that the angle between the symmetry axis and the cation-oxygen direction is 60° as detected in a recent spin echo study [29], and that the cation-oxygen direction is along the bisector of the water molecule, the metal-proton direction is at 8° away from $g_{\parallel}$ for the "axial" protons, and at 22° from $g_{\perp}$ for the "equatorial" protons. If all protons belong to water molecules, the contributions to the total ENDOR intensity of equatorial and axial protons should be equal. The ratio of 1:0.33 deduced from the simulations suggests that some of the oxygen ligands could be from the oxygens of undissociated sulfonic acid groups. From the present data it is not possible to specify the exact source of the ligating oxygens. We add that these conclusions are valid if the relaxation mechanism of all protons is approximately the same.

Fig. 7. Simulation of the ENDOR signals given in Fig. 4 (site 1 in Ti^{3+}/Nafion/water) with Lorentzian line shapes, and a line width of 0.45 MHz. The equatorial proton is at 2.60 Å, with $A_{iso} = 5.10$ MHz; the axial proton is at 3.10 Å, with $A_{iso} = -0.60$ MHz; the matrix proton is at 5.10 Å and $\theta_N = 0°$. (A) Separate contributions of the protons and the sum for the perpendicular field setting ($\theta_H = 90°$). (B) Separate contributions of the protons and the sum for the parallel field setting ($\theta_H = 0°$). (C) ENDOR spectra for the perpendicular and parallel field settings, showing the large splitting expected from the axial proton, that was not observed in the experimental spectra. In calculating the final spectra, the intensity ratio of the equatorial, axial and matrix protons is 1:0.33:0.75.

VI. Conclusions

The method of orientation-selected ENDOR has been applied to the study of Ti^{3+} solvation in methanol, and in Nafion perfluorinated membranes swollen by water and methanol. In site 1 of Ti^{3+} in methanol an axial **g**-tensor was measured, with $g_{\|} = 1.986$ and $g_{\perp} = 1.894$, suggesting a trigonally distorted octahedral symmetry. The distance of the cation to the methyl protons, is in the range 4.1 to 4.6 Å and no orientation selection is possible. In site 2 of Ti^{3+} in methanol the principal components of the **g**-tensor are $g_{\|} = 1.943$ and $g_{\perp} = 1.960$, suggesting a tetragonally distorted octahedral symmetry. Orientation selected ENDOR data and simulations indicate two types of methyl protons, at 4.35 Å (axial proton) and 3.95 Å (equatorial proton) from the cation. In Nafion swollen by water R_N values of 3.10 Å (for axial protons) and 2.60 Å (for equatorial protons) are suggested from orientationally selected ENDOR signals and simulations. The large splittings from OH group protons in the equatorial positions are not easily detected, most likely due to a range of distances to the cation and orientations with respect to the **g**-tensor directions.

Acknowledgements

This study was supported by NSF Grants DMR-8718947 (Polymer Program) and INT-8610708 (Cooperative Research US-Sweden). Acknowledgement is also made to the Donors of The Petroleum Research Fund, administered by the ACS, for partial support of this research. B.E.M. was supported in part by the NSF Research Experience for Undergraduate (REU) program. A particularly illuminating discussion with Didier Gourier (Paris) contributed greatly to our understanding of Ti^{3+} ENDOR.

[1] L. Kevan and L. D. Kispert, Electron Spin Nuclear Double Resonance Spectroscopy, Wiley-Interscience, New York 1976.
[2] H. Kurreck, B. Kirste, and W. Lubitz, Angew. Chem. Int. Ed. **23,** 173 (1984).
[3] K. Möbius and R. Biehl, Multiple Electron Resonance Spectroscopy, M. M. Dorio and J. K. Freed Eds. Plenum Press, New York 1979.
[4] H. Kurreck, B. Kirste, and W. Lubitz, Electron Nuclear Double Resonance Spectroscopy of Radicals in Solution, VCH Publishers, New York 1988.
[5] S. Schlick, L. Kevan, K. Toriyama, and M. Iwasaki, J. Chem. Phys. **74,** 282 (1981).
[6] A. Schweiger, Electron Nuclear Double Resonance of Transition metal Complexes with Organic Ligands, Springer-Verlag, Berlin 1982, p. 26.
[7] P. J. O'Malley and G. T. Babcock, J. Amer. Chem. Soc. **108,** 3995 (1986).
[8] a) G. C. Hurst, T. A. Henderson, and R. W. Kreilick, J. Amer. Chem. Soc. **107,** 7294 (1985); b). T. A. Henderson, G. C. Hurst, and R. W. Kreilick, J. Amer. Chem. Soc. **107,** 7299 (1985).
[9] D. Mustafi and M. W. Makinen, Inorg. Chem. **27,** 3360 (1988).
[10] A. Alagna, D. Attanasio, T. Prosperi, and A. A. G. Tomlinson, J. Chem. Soc. Faraday Trans. **85,** 689 (1989).
[11] S. Schlick, L. Sjöqvist, and A. Lund, Macromolecules **21,** 535 (1986).
[12] M. G. Alonso-Amigo and S. Schlick, J. Chem. Soc. Faraday Trans. 1 **83,** 3575 (1987).
[13] A. B. Brik, I. V. Matyash, and Yu Fedotov, Tverd. Tela **19,** 71 (1977) (in Russian).
[14] G. Labauze, J. B. Raynor, and E. Samuel, J. Chem. Soc. Dalton Trans. **12,** 2425 (1980).
[15] D. A. van Wezep, R. van Kemp, E. G. Severts, and C. A. Ammerlaan, Phys. Rev. B **32,** 7129 (1985).
[16] a) D. Gourier, D. Vivien, and E. Samuel, J. Amer. Chem. Soc. **107,** 7418 (1985); b) ibid. **109,** 4571 (1987).
[17] D. Gourier and E. Samuel, Inorg. Chem. **27,** 3018 (1988) and private communication.
[18] N. M. Atherton and J. F. Shackelton, Mol. Phys. **39,** 1471 (1980).
[19] H. van Willigen, C. F. Mulks, and N. M. Atherton, Inorg. Chem. **21,** 1708 (1982).
[20] G. A. Alonso-Amigo and S. Schlick, J. Phys. Chem. **90,** 6353 (1986).
[21] S. Schlick, G. A. Alonso-Amigo, and S. S. Eaton, J. Phys. Chem. **93,** 7906 (1989).
[22] M. G. Alonso-Amigo, Ph.D. Dissertation, University of Detroit, (1988).
[23] The program is available from the authors by request.
[24] a) J. E. Wertz and J. R. Bolton, Electron Spin Resonance, Chapman and Hall, New York 1986, p. 324; b) ibid. p. 277.
[25] H. C. Box, Radical Ionic Systems, A. Lund and M. Shiotani, Eds., Kluwer Press (1991).
[26] A. Lund and S. Schlick, Rev. Chem. Intermediates **11,** 37 (1989).
[27] I. B. Goldberg and W. F. Goepinger, Inorg. Chem. **11,** 3129 (1972).
[28] A. M. Chmelnick and D. Fiat, J. Chem. Phys. **51,** 4238 (1969).
[29] a) H. Tachikawa and T. Ichikawa, J. Amer. Chem. Soc. **112,** 977 (1990); b) ibid. **112,** 982 (1990).

Verantwortlich für den Inhalt: A. KLEMM
Satz und Druck: Konrad Triltsch, Würzburg